CHEMISTRY
A European Journal

A Journal of
ChemPubSoc Europe

Accepted Article

Title: A New Class of Lanthanide Complexes with three Ligand Centered Radicals: NMR Evaluation of Ligand Field Energy Splitting and Magnetic Coupling

Authors: Markus Hiller, Thomas Sittel, Hubert Wadepohl, and Markus Enders

To be cited as: *Chem. Eur. J.* 10.1002/chem.201901388

Link to VoR: http://dx.doi.org/10.1002/chem.201901388

Supported by
ACES

WILEY-VCH

10.1002/chem.201901388

A New Class of Lanthanide Complexes with three Ligand Centered Radicals: NMR Evaluation of Ligand Field Energy Splitting and Magnetic Coupling

Markus Hiller[1], *Thomas Sittel*[1], *Hubert Wadepohl*[1], *and Markus Enders**[1]

1 Institute of Inorganic Chemistry, Heidelberg University, Im Neuenheimer Feld 270, 69120 Heidelberg, Germany

* To whom correspondence should be addressed. Tel: +49-6221-546247, Fax: +49-6221-541616247, E-mail: markus.enders@uni-heidelberg.de

10.1002/chem.201901388

ABSTRACT

Combination of three radical anionic Ph-BIAN ligands (Ph-BIAN = bis-(phenylimino)-acenaphtenequinone) with Lanthanoid ions leads to a series of homoleptic, six-coordinate complexes of the type $Ln(Ph\text{-}BIAN)_3$. Magnetic coupling data were measured by paramagnetic solution NMR spectroscopy. Combining ^{1}H NMR with ^{2}H NMR of partially deuterated compounds allowed a detailed study of the magnetic susceptibility anisotropies over a large temperature range. The observed chemical shifts were separated into ligand- and metal-centered contributions by comparison with the Y analogue (diamagnetic at the metal). The metal-centered contributions of the complexes with the paramagnetic ions could then be separated into pseudocontact and Fermi contact shifts. The latter is large within the Ph-BIAN scaffold, which shows that magnetic coupling is significant between the lanthanide ion and the radical ligand. Pseudocontact shifts were further correlated to structural data obtained from X-ray diffraction experiments. Ligand field parameters were determined by fitting the temperature dependence of the observed magnetic susceptibility anisotropies. The electronic structure determined by this approach shows, that the Er and Tm analogues are candidates for single molecule magnets (SMM). These results demonstrate the possibilities for the application of NMR spectroscopy in investigations of paramagnetic systems in general and single molecule magnets in particular.

10.1002/chem.201901388

INTRODUCTION

Single molecule magnets (SMMs) are a class of compounds capable of retaining molecular magnetization below a certain blocking temperature T_B. In order to achieve this behavior, a bistable ground state is necessary, combined with a preferably large thermal barrier preventing the flip of the magnetization. While the effect was first discovered in *d* metal compound ("$Mn_{12}OAc$")[1], in recent years lanthanide ions have increasingly entered the focus of research and SMM behavior was observed for compounds featuring only a single paramagnetic ion.[2] In contrast to many d metal compounds the lanthanide ions feature large orbital contributions to the total angular momentum of the unpaired electrons, in particular in the second half of the series (Tb^{3+}–Yb^{3+}), where spin-orbit-coupling is additive. The key factor for achieving bistability in lanthanide based SIMs is the ligand field which removes the degeneracy of the *2J+1* microstates.[3] Depending on the specific geometry and the type of ligand, this splitting may favor microstates with highest, intermediate or even lowest possible m_J values. Furthermore, this preference depends on the ion and thus for a given ligand field environment only certain ions are suitable candidates for SMMs.[3a] Attempts have been made to categorize the lanthanide ions into oblate and prolate ones, based on the asphericity of their *f* electron density.[4] While this approach is beneficial for the quick selection of promising candidates and has been applied successfully in the discovery of the best-performing SMM system to date, it neglects that due to ligand field effects the shape of the free ion ground state may not reflect that of the m_J state of lowest energy in a coordination compound. Hence, the prolate or oblate character of a particular ion is subject to the influence of the ligand field. One prominent example for this behavior is Dy^{3+} (*J = 15/2*) in $[DyCp_2]^+$, $DyPc_2$ and $[Dy(COT)_2]^-$ systems (Cp = substituted cyclopentadienide, Pc = Phtalocyaninato, COT = cyclooctatetraene). While in the first two cases the ground state is considered to be predominantly |±13/2> (oblate)[5], it is assumed to be |±9/2> (weakly prolate) in the latter.[6] This illustration demonstrates that insight into the electronic structure of the lanthanide ions is of paramount importance in the field of SMM research. Consequently, the theoretical treatment of such systems by means of CASSCF calculations is developing rapidly.[7] On the other hand there are also experimental

methods like SQUID magnetometry as well as torque magnetization measurements,[8] which provide helpful information. It has been demonstrated that NMR techniques can be included as well,[5, 9] yet examples for their application are sparse. In this report we want to demonstrate how NMR spectroscopy alone can be used as a tool for the determination of magnetic parameters and the identification of promising SMM candidates. We have therefore investigated a previously unknown series of homoleptic lanthanide complexes featuring three monoanionic radical ligands.

The enforcement of desired coordination geometries of lanthanide ions is far more challenging than in the case of *d* group metals. Reasons for this are the comparatively large radii and the strong Lewis acidity. Thus, high coordination numbers are commonly observed, often combined with irregular coordination polyhedra. While these observations by no means preclude SMM behavior, they are in contrast to the comparatively highly symmetric ligand fields encountered in many high-performing lanthanide SIMs.[7b] We have therefore intended to achieve highly symmetric coordination of the lanthanide ions in combination with a relatively small coordination number of six. In addition to that, we envisaged to use ligands containing unpaired electrons themselves in order to study the magnetic coupling phenomena within the ligand scaffold and between ligand and metal centered unpaired electrons. Such couplings are important for opening magnetic hysteresis loops as has been shown recently by a number of papers.[10]

RESULTS

A new group of neutral lanthanide complexes was synthesized by combining a Ln^{3+} ion with three bidentate, monoanionic bis-(phenylimino)-acenaphtenequinone (Ph-BIAN) ligands. This ligand was first described in 1967[11] and can be converted to its radical anion by addition of one equivalent of alkali metal[12] (potassium was used herein). The resulting intensely green metal salt can be isolated or reacted *in situ* with anhydrous $LnCl_3$ in tetrahydrofuran at room temperature or at elevated temperature in toluene. To the best of our knowledge, the reaction of this ligand with lanthanide

10.1002/chem.201901388

halogenides has so far not been reported in a 3:1 stoichiometry.[13] Notably, similar vanadium complexes with a related ligand have been described previously.[14]

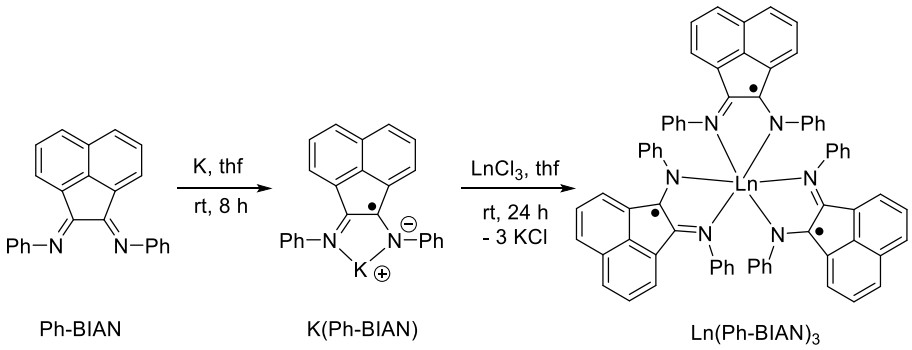

Ln=		
Y^{3+}	**1**	71 %
Gd^{3+}	**2**	80 %
Tb^{3+}	**3**	56 %
Dy^{3+}	**4**	93 %
Ho^{3+}	**5**	67 %
Er^{3+}	**6**	97 %
Tm^{3+}	**7**	92 %

Scheme 1: Synthesis of the Ln(Ph-BIAN)$_3$ compounds and isolated yields.

As summarized in scheme 1, the Ln(Ph-BIAN)$_3$ compounds were obtained in high yields. Due to their neutral charge, they are soluble in common organic solvents and can therefore be isolated by extraction with toluene as intensely red solids. The stoichiometry of the reaction should be met exactly to avoid the formation of toluene-soluble byproducts. The compounds are very sensitive to air and moisture, particularly in solution, and have to be handled accordingly. All compounds were characterized by NMR spectroscopy and elemental analysis. The reaction sequence was further carried out using a partially deuterated ligand (prepared from aniline-D_5, for details see ESI). This allowed the independent identification of the NMR signals arising from the acenaphthene backbone and the phenyl groups. As the NMR relaxation rate in paramagnetic compounds depends on the gyromagnetic ratio of the investigated nucleus, ^{2}H gives much smaller line widths compared to ^{1}H, which in turn facilitates the detection of the NMR signals.[15] Furthermore, the fact that ^{2}H has a quadrupole moment opens the possibility of gaining structural geometric information from residual quadrupolar couplings (see below).[16]

Single crystals of the toluene solvate Ho(Ph-BIAN)$_3$·2 C_7H_8 were obtained from a toluene solution and the solid-state molecular structure was determined by X-ray crystallography (see Figure 1, left). In the

10.1002/chem.201901388

crystals, Ho(Ph-BIAN)$_3$ attains C_2 point symmetry. However, the molecular structure is close to D_3 symmetry as evidenced by the corresponding bond lengths and angles. The length of the acenaphthene backbone carbon carbon bond C1-C2 [C25-C25', respectively] can be used as a measure for the redox state of the ligands and is found to be 1.445(2) [1.446(3)] Å, which is in line with reported values for a mono-anion.[12]

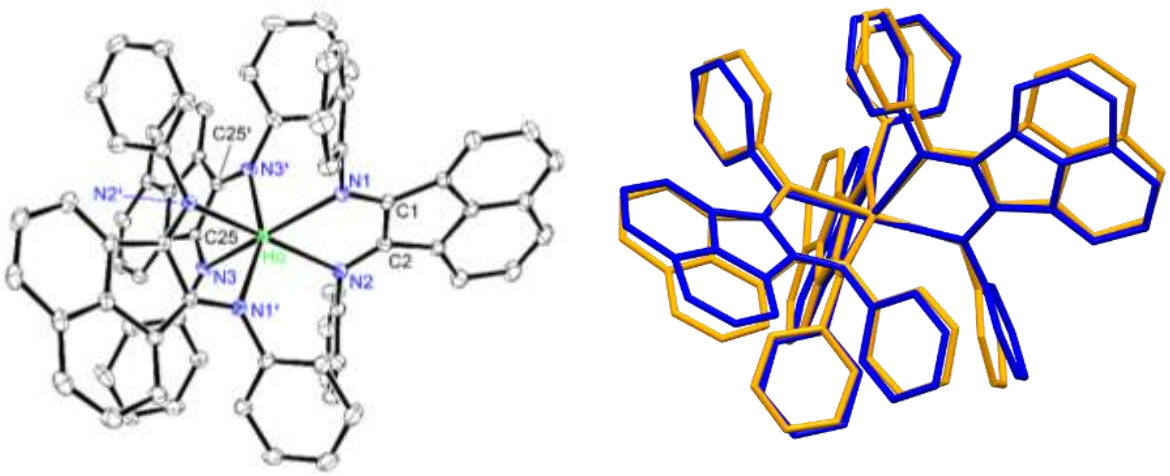

Figure 1: Left: Molecular structure of Ho(Ph-BIAN)$_3$·2 C_7H_8. Hydrogen atoms and co-crystallized toluene are omitted for clarity; displacement ellipsoids are drawn at the 50% probability level. Selected bond lengths and angles: Ho-N1: 2.3519(14), Ho-N2: 2.3792(14), Ho-N3: 2.3736(15) Å, N1-Ho-N2: 70.60(5), N3-Ho-N3': 71.04(7), N1-Ho-N3': 93.39(5), N1-Ho-N2': 103.43(5), N2'-Ho-N3': 93.86(5). Right: Overlay of the solid-state structure of Ho(Ph-BIAN)$_3$ (orange) and a model with enforced D_3 symmetry (blue).

The solution structure was explored further by DFT-optimization of the Y analogue. Y^{3+} was chosen as it does not contribute to the paramagnetism of the molecule and has an ionic radius close to Ho^{3+} (Y^{3+}: 115.8 pm, Ho^{3+}: 115.5 pm for eight-fold coordination),[17] which places it in the center of the investigated series. The comparison of the solid-state structure of Ho(Ph-BIAN)$_3$ and the structure of **1** with enforced D_3 symmetry (Figure 1, right) demonstrates that only small structural changes result in a significantly higher symmetry. Moreover, almost no variation of the atom positions of the first coordination sphere is required.

10.1002/chem.201901388

NMR Analysis

From the perspective of NMR spectroscopy the combination of three organic radical ligands with a paramagnetic metal ion may appear disadvantageous, as organic radicals are usually difficult to study by NMR due to their very broad resonance lines. Line widths in NMR spectra of paramagnetic molecules are strongly influenced by the electron relaxation rate.[18] Slow electron relaxation as commonly observed in organic radicals or transition ions with half-filled shells (*e.g.* Mn^{2+}, Gd^{3+}), causes extremely fast relaxation of the NMR nuclei, usually increasing the NMR line widths beyond the detection limit. However, if the organic radical is combined with a paramagnetic metal ion, the unpaired electrons at the metal influence the relaxation of the ligand unpaired electron. This increases the electron relaxation rates and in turn reduces the line broadening of the NMR nuclei. At the same time, the interaction of the NMR nuclei with unpaired electrons of the metal leads to additional line broadening. However, if the metal ion exhibits high electron relaxation rates, the overall line broadening is smaller compared to NMR signals of purely ligand based paramagnetic compounds. Consequently, the NMR detectability of organic radicals can be improved by coordinating them to paramagnetic metal ions. The system studied here, presents an example of this case, which is evidenced by the fact that NMR line widths are significantly larger for the analogous Y complex, with some signals being undetectable (see below).

The ^{1}H NMR spectra of the series Tb^{3+} – Tm^{3+} in toluene-d_8 consist of only four relatively sharp signals at room temperature with equal integrals. However, six or eight signals would be expected depending on whether the rotation of the phenyl groups is fast or slow on the NMR timescale. The presence of only four signals is due to the disappearance of the *ortho*- and *meta*-protons of the phenyl groups caused by intermediate fast rotation of the phenyl rings with coalescence near room temperature. At higher temperatures two new signals appear whereas at lower temperatures these split into four signals (see Figures S5 and S6). The excellent solubility of the compounds was exploited for a detailed measurement of the temperature dependence of the NMR shifts covering the range from 235 K to 365 K.

10.1002/chem.201901388

In the case of the Y^{3+} analogue **1** four broad signals are observed as well. However, three of them stem from the phenyl ring whereas only one ^{1}H resonance of the three H atoms from the acenaphthene moiety can be observed. In this compound, the phenyl ring rotation is fast on the NMR time scale because the chemical shift difference of the interconverting H atoms (*ortho*-phenyl and *meta*-phenyl, respectively) is small due to the absence of lanthanide-centered pseudocontact shift. This interpretation is supported by the ^{2}H NMR of the deuterated analogue where three signals from the phenyl rings are present at room temperature. On the other hand, the unfavorable NMR relaxation properties of organic radicals lead to significant line broadening of the resonances of the ^{1}H atoms in the acenaphthene group so that only one (H^4) out of three NMR signals is observable (see Fig. 3).

1 provides the possibility to investigate the interaction among the three radical ligands. If their spins are oriented parallel, a quartet spin state results whereas an anti-parallel orientation gives a spin-frustrated doublet state. Which of the two possibilities is lower in energy depends on whether the spin-spin coupling interaction is ferromagnetic or antiferromagnetic in nature.

The ^{1}H NMR spectrum of $Y(Ph\text{-}BIAN)_3$ (Figure S1,) changes only slightly with temperature, in analogy to the description of a related vanadium complex featuring highly similar ligands.[14] This behavior disagrees with a pure doublet or quartet state, for which a T^{-1} dependence of the chemical shifts is expected. However, the observed temperature dependence is in agreement with a doublet ground state and quartet state close in energy. Upon increase of the temperature, the Boltzmann occupancy of the quartet state increases, for which higher chemical shifts occur resulting from the larger number of unpaired electrons. Simultaneously, the T^{-1} dependence of the chemical shifts of both the ground and excited states counteracts this variation, leading to only minor net changes of the observed spectra. The fit of the observed chemical shifts provided a value of 288.0 ± 4.5 cm^{-1} for the energy separation in favor of the doublet state. This corresponds to an antiferromagnetic coupling constant of $J = -(96 \pm 1.5)$ cm^{-1}, resulting in a nearly linear increase of the occupancy of the quartet state from 14.7 % to 24.2 % in the investigated temperature range. In addition, the ligand-based Fermi contact contributions associated with both spin states were obtained from the fitting procedure, which is

10.1002/chem.201901388

described in more detail in the ESI. In order to assign the signals, the spin densities for the respective nuclei were derived from DFT calculations of Y(Ph-BIAN)$_3$. For this purpose, four different functionals (B3LYP, TPSSh, PBE and BP86) were employed in geometry optimizations of the complex in both spin states. The largest proton spin densities were in all cases found for the H^3 and H^5 positions (compare Figure 2). As a consequence, fast relaxation broadens the NMR signals of these nuclei beyond the detection limit. For the H^4 and H^{10} nuclei positive spin densities were calculated while the respective values are negative for H^9 and H^{11}, agreeing with the recorded NMR spectrum of **1** (Figure 2). Comparison with the spectrum of the partially deuterated analogue allowed the distinction of H^4 and H^{10}, while the lower relative integral of H^{11} allows the differentiation from H^9.

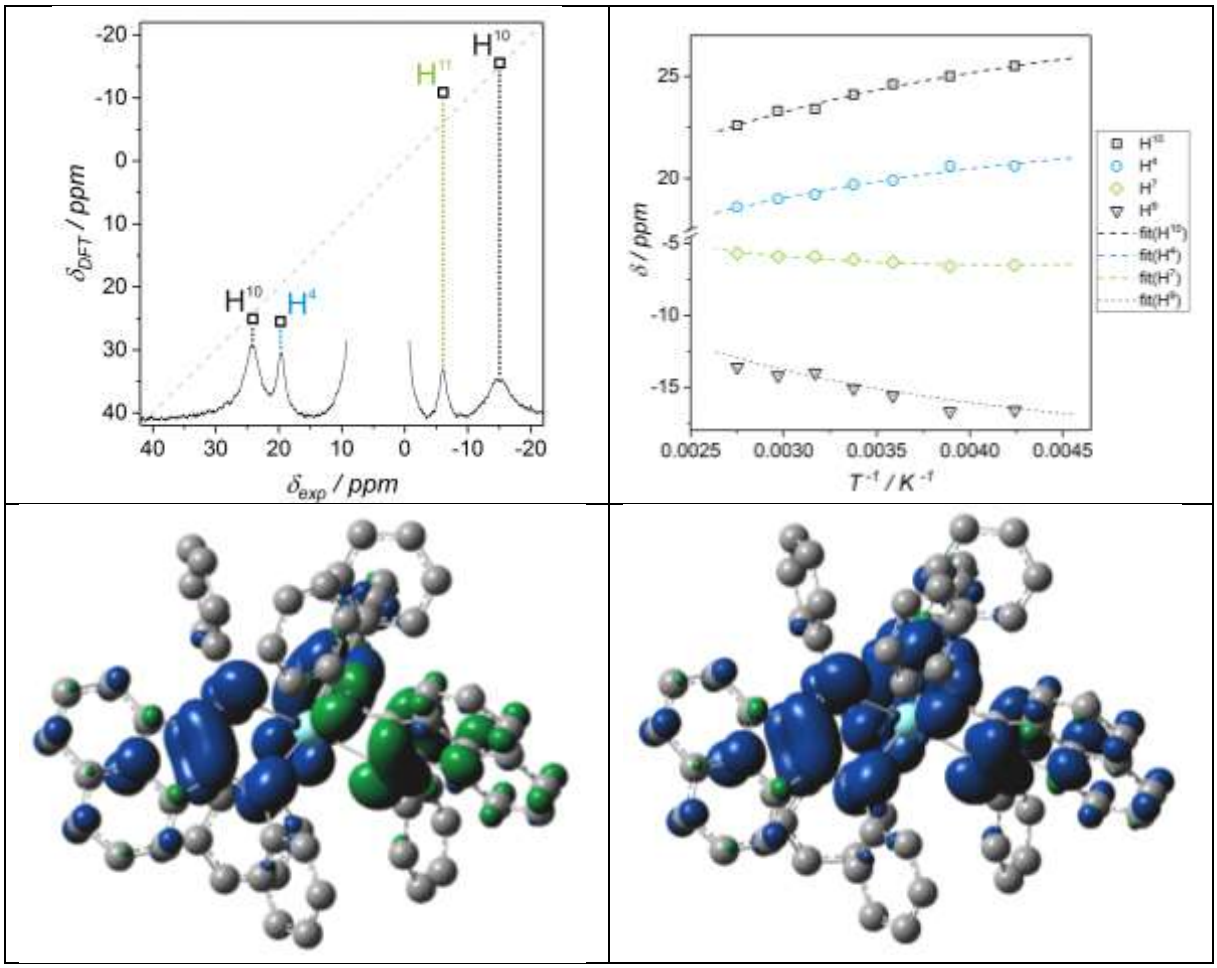

Figure 2: Top left: Calculated (DFT, TPSSh) versus experimental chemical shifts of **1** at 296.2 K containing 19.5 % of the quartet state. Top right: Comparison of the temperature-dependent chemical shifts of **1** and the values fitted corresponding to a coupling constant of J = −96 cm^{-1}. Values are plotted against the inverse temperature to emphasize the deviation from Curie behavior. Bottom: Spin density distribution of the doublet (left) and quartet (right) spin states of **1**.

10.1002/chem.201901388

Valuable information about the magnetic anisotropies of the respective lanthanide ions can be extracted from the NMR spectra. The observed chemical shifts are influenced by the paramagnetism of both the radical anions and the lanthanide ions. Both contributions can be separated into a Fermi-contact and a pseudocontact shift.[19] The complete description is given in Eq. 1.

$$\delta_{obs}^{i,j} = \delta_{orb}^{i} + \delta_{lfc}^{i} + \delta_{lpc}^{i} + \delta_{mfc}^{i,j} + \delta_{mpc}^{i,j} \quad (1)$$

The observed chemical shift $\delta_{obs}^{i,j}$ of a nucleus *i* in the complex of lanthanide *j* thus consists of the orbital shift contribution δ_{orb}^{i}, the ligand-based Fermi-contact-contribution δ_{lfc}^{i} as well as the ligand-based pseudocontact contribution δ_{lpc}^{i} and, finally, the metal-based Fermi-contact $\delta_{mfc}^{i,j}$ and pseudocontact shift $\delta_{mpc}^{i,j}$. Please note, that the analysis in this way assumes a simple additive behavior of all shift contributions. In order to extract information about the magnetic properties of the lanthanide ion, in particular the magnetic anisotropy, the separation of the individual shifts is necessary. The sum of the first three terms in eq. 1 corresponds to a system without unpaired f-electrons (i.e. the Y^{3+}, La^{3+} or Lu^{3+} derivatives). The larger (or smaller, respectively) ionic radii of La^{3+} and Lu^{3+} as compared to the series from Tb^{3+} to Tm^{3+} leads to considerable differences in the inter-ligand distances, thus significantly modifying the size of the magnetic coupling between the ligands. The presence of energetically accessible f-electrons should not influence the interligand coupling seriously, as f orbitals are shielded rather effectively by the more outward-lying, larger d orbitals. The size of the Y^{3+} ion is in the middle of the investigated series (Tb^{3+} to Tm^{3+}) and thus we choose complex **1** as reference system. Therefore, eq. 1 can be rewritten as eq. 2.

$$\delta_{obs}^{i,j} = \delta_{obs}^{i,Y} + \delta_{mfc}^{i,j} + \delta_{mpc}^{i,j} \quad (2)$$

The metal-based pseudocontact shift $\delta_{mpc}^{i,j}$ of a lanthanide ion *j* is described with Eq. 3 for an axial system.[20] This contribution depends on the axial anisotropy of the magnetic susceptibility ($\Delta\chi_{ax}^{j}$) as well as the metal-nucleus distance r_i and the polar angle θ_i of the metal-nucleus vector with respect to the magnetic main axis. This geometric information is often combined in the geometrical factor G^i.

$$\delta_{mpc}^{i,j} = \frac{1}{12\pi} \cdot \Delta\chi_{ax}^{j} \cdot \frac{(3cos^2\theta_i - 1)}{r_i^3} = \frac{1}{12\pi} \cdot \Delta\chi_{ax}^{j} \cdot G^i \quad (3)$$

For compounds **2 – 7** we assume that the effective magnetic main axis lies along the approximated molecular C_3 axis. This assumption is in line with previous calculations for lanthanide ions in trigonal-prismatic environments.[21] Tilting of the axis should produce a higher number of NMR signals unless these are averaged by rotation. This process would influence individual nucleus positions in a different way due to the angular and radial dependence of the geometric factor. Consequently, if all metal-centered pseudocontact shifts $\delta_{mpc}^{i,j}$ of a specific lanthanide ion can be simultaneously fitted to a set of geometric factors G^i of a geometric model (calculated with respect to a specific magnetic main axis) and a single $\Delta\chi_{ax}^{j}$ value, the direction of the effective magnetic axis is correct. It is further assumed that the contraction of the ionic radii along the investigated series is negligibly small, so that all compounds can be described by the same set of geometrical factors G^i.

The metal-based Fermi contact shift $\delta_{mfc}^{i,j}$ is expressed by eq. 4 involving the reduced average spin polarization $\langle S_z \rangle$.[22] The shift further depends on the temperature T, the gyromagnetic ratio γ^j of the investigated nucleus and the hyperfine coupling constant $A^i/\hbar$ for this nucleus (in units of rad·s^{-1}); μ_B represents the Bohr magneton and k is Boltzmann's constant.

$$\delta_{mfc}^{i,j} = \frac{\mu_B}{3kT\gamma_i} \cdot \frac{A^i}{\hbar} \cdot \langle S_z \rangle^j \quad (4)$$

$\delta_{mfc}^{i,j}$ is usually small for most nuclei in Lanthanide compounds, as the unpaired electrons are located within *f*-orbitals that do interact only weakly with the ligand atoms. Therefore, this contribution is often disregarded, however, the presence of the radical ligands may enhance spin delocalization between *f*-centered and ligand centered unpaired electrons. Accordingly, we included this contribution in our analysis and combined eqs. 2, 3 and 4 to eq. 5:

$$\delta_{obs}^{i,j} = \delta_{obs}^{i,Y} + \frac{\mu_B}{3kT} \cdot \frac{A^i}{\hbar} \cdot \langle S_z \rangle^j + \frac{1}{12\pi} \cdot \Delta\chi_{ax}^{j} \cdot G^i \quad (5)$$

10.1002/chem.201901388

As the susceptibility anisotropies of the different lanthanide ions are of particular importance, a second methodology to obtain their values was employed by investigation of the ^{2}H NMR spectra of the analogous complexes bearing partially deuterated ligands. Due to the large magnetic anisotropy a partial orientation of the molecules in magnetic fields is induced. In the case of nuclei with quadrupole moments (nuclear spin $I > ½$) this leads to a splitting of the observable signal into $2 \cdot I$ lines, *i.e.* a doublet in the case of ^{2}H.[16, 23] The size of the splitting is described by Eq. 6.

$$\left|\Delta\nu_Q\right| = \frac{(B_0)^2}{20\mu_0 kT} \cdot \frac{e^2qQ}{h} \cdot \left|(3cos^2\phi - 1) \cdot \Delta\chi_{ax}\right| \quad (6)$$

In this expression B_0 represents the applied magnetic flux density and μ_0 is the vacuum permeability. The second factor e^2qQ/h is the nuclear quadrupole coupling constant of deuterium, which differs slightly depending on the specific environment. Suitable values can be found in the literature and herein a value of 186 ± 6 kHz has been used.[24],[25],[26] Similar to eq. 3 an angular dependence is encountered. In this case, however, the angle of interest is measured between the magnetic main axis and the electric field gradient surrounding the investigated nucleus. As each deuterium nucleus is bound to only one carbon atom, the latter lies along the direction of the C–^{2}H bond. The partial orientation depends on the susceptibility anisotropy of the entire molecule, including diamagnetic and paramagnetic contributions from the ligands. However, the ligand contributions to the total magnetic anisotropy of the series is negligible, as the ^{2}H NMR spectrum of **1** does not show a splitting or in other words the RQC splitting in **1** is considerably smaller than the line width of the observed ^{2}H resonance line (ca. 40 Hz at 296 K, Lorentzian line shape).

Signal assignment

In order to obtain useful information, the correct assignment of the observed signals is required. Due to the different contributions that are not easily estimated, this process is far from trivial but can be achieved by some general considerations. Firstly, as described above, one of the observed signals

10.1002/chem.201901388

belongs to the proton in *para*-position of the phenyl group (H^{11}, see Fig. 3). The signal of this nucleus in the different complexes is easily identified by comparison with the ^{2}H NMR spectra. The NMR shifts of nuclei which are several bonds apart from the lanthanide ions are usually dominated by the pseudocontact contribution, which is proportional to the susceptibility anisotropies of the individual lanthanide ions. However, due to the unpaired electron in the BIAN scaffold, a stronger delocalization of unpaired f-electron density to the ^{1}H atoms in the BIAN backbone has to be considered. As shown below this contribution may exceed 30 ppm for atoms H^3 and H^5. Nonetheless, pseudocontact dominates the shift of H^{11} due to its large distance (in terms of bonds) from the lanthanide ion and the non-participation of the phenyl group in ligand unpaired electron delocalization. The geometric factor *G* for H^{11} is positive and consequently large positive NMR shifts for this nucleus correspond to large positive $\Delta\chi_{ax}^{j}$ values and vice versa. Therefore, an arrangement of the spectra in the order of increasing chemical shift for the H^{11} proton (Fig. 3) represents the decreasing order of the $\Delta\chi_{ax}^{j}$ values. This order is found to be $Tb^{3+} < Dy^{3+} < Ho^{3+} < Er^{3+} < Tm^{3+}$, which is consistent with values predicted by the literature for this coordination polyhedron.[21] Comparison with the spectra of $Y(Ph\text{-}BIAN)_3$ shows, that the $\Delta\chi_{ax}^{j}$ values switch signs between Ho^{3+} and Er^{3+}, which is in line with the classification of oblate and prolate ions as well as the values predicted for this coordination geometry.[4b, 21]

10.1002/chem.201901388

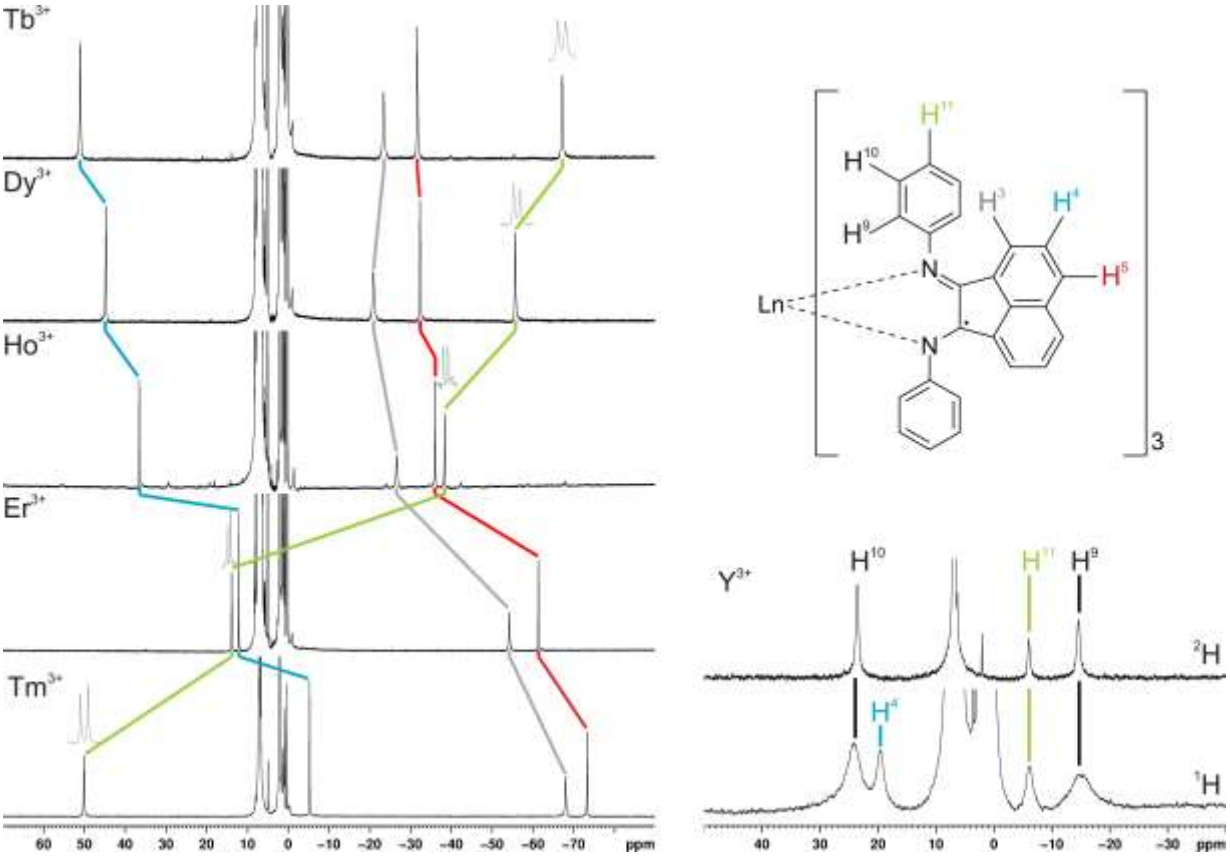

Figure 3: Left: overlay of ^{1}H NMR spectra (15.1 T, 296 K, toluene-d_8) of the Ln(Ph-BIAN)$_3$ compounds (top to bottom: Ln = Tb^{3+}, Dy^{3+}, Ho^{3+}, Er^{3+} and Tm^{3+}) with expansions showing the RQC splitting of the ^{2}H NMR signal of D^{11} in the partially deuterated analogues **3D$_{30}$.– 7D$_{30}$** Colored lines illustrate the shifts of the signals arising from identical nuclei. Top right: Labeling scheme for the compounds with colored positions corresponding to the signals in the NMR spectra. Bottom right: Stacked ^{1}H and ^{2}H NMR spectra (15.1 T, 296 K, toluene-d_8) of **1** and **1D$_{30}$**.

10.1002/chem.201901388

From this arrangement it is easily found, that the remaining signal exhibit similar shift patterns. However, due to the different geometrical factors of these nuclei, the strength and direction of the shift variations differs. The line widths of the signals support the observed patterns, which is most clearly seen in the signals of the H^3 group as these are the broadest for all lanthanide ions. It must be noted, that the signal of H^3 in Tb(Ph-BIAN)$_3$ does notably deviate from the otherwise regular pattern. This effect is a result of a sizeable metal-based Fermi contact shift. The simultaneous fitting of all ^{1}H NMR signals as described below leads to a separation of metal centered Fermi-contact and pseudocontact shifts. The result for the complex Tb(Ph-BIAN)$_3$ is presented in figure 4 (for charts of the other complexes see the Supporting Information). Large Fermi-contact shifts induced by the unpaired f-electrons is distributed onto the BIAN scaffold (mainly on H^3 and H^5) whereas H^{11} at the phenyl substituent carries only very small contact shifts.

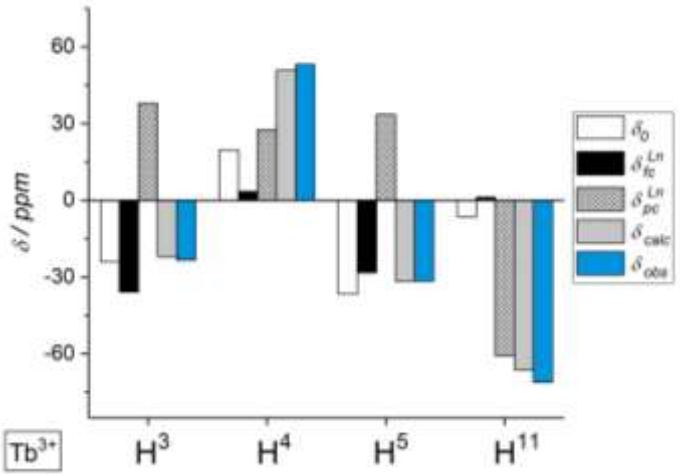

Figure 4: Shift contributions for Tb(Ph-BIAN)$_3$ at 296.2 K with δ_0 = shift of Y(Ph-BIAN)$_3$, δ_{fc} = metal induced Fermi-contact shift, δ_{pc} = metal induced pseudocontact shift, δ_{calc} = shift resulting from fitting, δ_{obs} = observed chemical shift.

All observable ^{1}H NMR shifts were simultaneously fitted to an alternative expression of Eq. 5, as described previously for substituted lanthanide-cyclooctatetraene systems.[20b, 22b, 27] For this purpose, the geometric factors G^i are replaced by relative geometric factors G'^i (see ESI for details), which is fixed to unity for one nucleus chosen arbitrarily. Simultaneously, only relative magnetic susceptibility

10.1002/chem.201901388

anisotropies result. This treatment allows the analysis of the NMR shifts without presuming structural information apart from isostructurality. The resulting relative geometric factors can then be compared for different geometric models and used for exploring the solution averaged structure. Once a suitable model has been identified, its geometric factors G^j can be used to translate the relative magnetic susceptibility anisotropies to the physically meaningful $\Delta\chi_{ax}^j$ values. The relative geometric factors obtained from the fitting (ESI, Table S.14) were compared to the values obtained from the solid-state structure of Ho(Ph-BIAN)$_3$ (Fig. 5, right). The ligand situated on the molecular C_2 axis has very similar geometric factors as obtained by the NMR fitting procedure. Thus, the NMR determined solution molecular structure of these paramagnetic complexes is very similar to the results of the X-ray diffraction. Accordingly, the susceptibility anisotropies $\Delta\chi_{ax}^j$ of the individual lanthanide ions were calculated from the relative values (ESI, Table S.15) and they correspond in an excellent way to the results of the analysis of the RQC splittings as well as the predictions by Mironov *et al.*[21] (Table 1, Fig. 5, left).

Table 1: Values of $\Delta\chi_{ax}^j$ for the individual lanthanide ions in Ln(Ph-BIAN)$_3$ at different temperatures obtained by the fitting procedure.

	$\Delta\chi_{ax}$ [10^{-31} m^3]						
	235.8 K	256.8 K	278.8 K	296.2 K	315.6 K	336.7 K	363.6 K
Tb^{3+}	−9.43 ± 2.54	−8.33 ± 2.23	−7.36 ± 1.96	−6.73 ± 1.77	−6.09 ± 1.56	−5.48 ± 1.37	−4.88 ± 1.18
Dy^{3+}	−8.48 ± 2.03	−7.53 ± 1.83	−6.67 ± 1.63	−6.11 ± 1.52	−5.56 ± 1.41	−5.03 ± 1.33	−4.48 ± 1.22
Ho^{3+}	−6.06 ± 1.55	−5.20 ± 1.33	−4.46 ± 1.11	−3.98 ± 0.98	−3.53 ± 0.85	−3.09 ± 0.73	−2.69 ± 0.62
Er^{3+}	3.13 ± 0.80	2.85 ± 0.66	2.54 ± 0.59	2.33 ± 0.55	2.03 ± 0.51	1.85 ± 0.49	1.62 ± 0.45
Tm^{3+}	9.38 ± 2.39	8.34 ± 2.00	7.28 ± 1.65	6.63 ± 1.45	5.83 ± 1.28	5.24 ± 1.15	4.61 ± 1.00

10.1002/chem.201901388

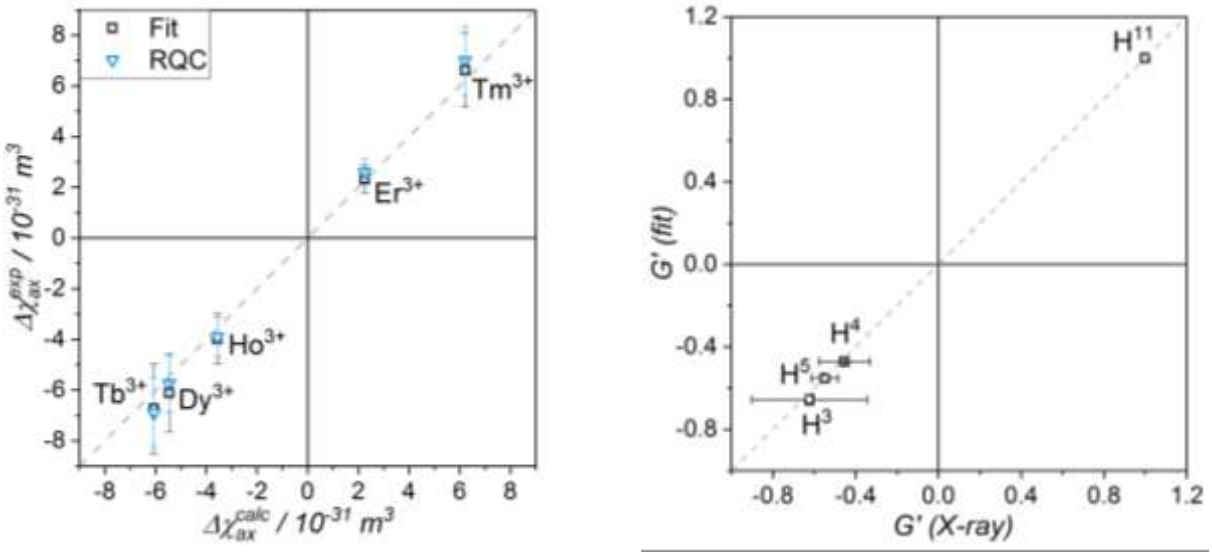

Figure 5: Left: Comparison of $\Delta\chi_{ax}^{j}$ values from the fitting procedure (black) and the RQC splittings (blue) with the values predicted in the literature.[21] Right: Comparison of relative geometric factors obtained from the fitting procedure with those calculated from one of the ligands in the solid-state structure of Ho(Ph-BIAN)$_3$.

Determination of Ligand field parameters

The low number of observable NMR signals indicates, the solution structure of the Ln(Ph-BIAN)$_3$ compound series to be of higher symmetry than C_2, as inferred from the solid-state structure of the Ho analogue. The comparison with a D_3 symmetric model (Figure 1) shows only minor deviations. Considering only the first coordination sphere (*i.e.* the nitrogen donor atoms) an almost perfect agreement of both structural models is found. Accordingly, a distorted trigonal prism is observed as the coordination polyhedron of the lanthanide ions, which conforms to the point group D_{3d}. The associated ligand field Hamiltonian[28] is given in the operator equivalent[29] form in Eq. 7. Apart from the three axial parameters B_k^0 (with k = 2,4,6) an additional parameter B_6^6 is encountered, leading to a mixing of the different m_J states in the ground state wave functions ψ_i.

$$\hat{H}_{LF}^{D_{3d}} = B_2^0\hat{O}_2^0 + B_4^0\hat{O}_4^0 + B_6^0\hat{O}_6^0 + B_6^6\hat{O}_6^6 \qquad (7)$$

The parameters B_k^q are composed of the ligand field parameters $A_k^q\langle r^k\rangle$ and the Stevens parameters[3a] k_{Jk}, specific for the lanthanide ions, as described by Eq. 8.

10.1002/chem.201901388

$$B_k^q = A_k^q \langle r^k \rangle \cdot k_{Jk} \tag{8}$$

For the determination of the ligand field parameters the approach recently applied in substituted bis-cyclooctatetraenyl lanthanide double decker compounds was adapted.[30] By diagonalization of the energy matrices, the contributions of the various m_J states to the wave functions ψ_i and their relative energies were obtained. Subsequently, the magnetic susceptibility tensor components were calculated using Eq. 9.[21, 31] Therein, the index *p* represents the direction in the magnetic axis system, *i.e.* either *x*, *y* or *z*, $\hat{J}_p$ is the associated total angular momentum operator and E_i is the relative energy of ψ_i.

$$\chi_p^{calc} = \frac{\mu_0 \mu_B^2 g_J^2}{2kT} \cdot \frac{\sum_i \left[\langle \psi_i | \hat{J}_p | \psi_i \rangle \langle \psi_i | \hat{J}_p | \psi_i \rangle - 2kT \cdot \sum_{j \neq i} \frac{\langle \psi_i | \hat{J}_p | \psi_j \rangle \langle \psi_j | \hat{J}_p | \psi_i \rangle}{E_i - E_j} \right] \cdot e^{(-E_i/kT)}}{\sum_i e^{(-E_i/kT)}} \tag{9}$$

Finally, calculated values for the axial anisotropies of the magnetic susceptibility ($\Delta\chi_{ax}^{calc}$) can be obtained according to the definition in Eq. 10 for the different lanthanides *j*.

$$\Delta\chi_{ax}^{j,calc} = \chi_z^{j,calc} - \frac{1}{2}\left(\chi_x^{j,calc} + \chi_y^{j,calc}\right) \tag{10}$$

Ligand field parameters were obtained by minimization of the root-mean-square deviation of calculated ($\Delta\chi_{ax}^{j,calc}$) and experimental anisotropies ($\Delta\chi_{ax}^{j}$). Following the approach used in the literature[5, 9] a linear variation of the parameters $A_k^q \langle r^k \rangle$ with the atomic number was imposed, reducing the number of parameters for the five investigated ions from 20 to 8. For the numeric calculations a custom-written script running in Octave 4.2 was used. A more detailed description of the fitting procedure and the script file can be found in the ESI. The results are presented in Table 2.

10.1002/chem.201901388

Table 2: Ligand field parameters for the individual ions obtained by the fitting procedure.

Parameter (cm^{-1})	Tb^{3+}	Dy^{3+}	Ho^{3+}	Er^{3+}	Tm^{3+}
$A_2^0\langle r^2\rangle$	−381 ± 7.6	−422 ± 10	−463 ± 13	−504 ± 15	−544 ± 17
$A_4^0\langle r^4\rangle$	−95 ± 3.8	−107 ± 5.1	−120 ± 6.3	−133 ± 7.6	−146 ± 8.9
$A_6^0\langle r^6\rangle$	−52 ± 2.6	−56 ± 3.6	−60 ± 4.5	−63 ± 5.4	−67 ± 6.4
$A_6^6\langle r^6\rangle$	850 ± 17	1008 ± 22	1165 ± 26	1323 ± 31	1480 ± 36

The obtained parameters result in excellent agreement of the observed and calculated anisotropies as demonstrated in Fig. 6. Most notably, the primary parameter $A_2^0\langle r^2\rangle$ is determined to be negative for the Ln(Ph-BIAN)$_3$ compounds series, indicating a predominantly equatorial ligand field. The large $A_6^6\langle r^6\rangle$ parameter results in a pronounced mixing of different m_J states with $\Delta m_J = 6$ in the ground state wave functions ψ_i (see Tables S.36–S.40).

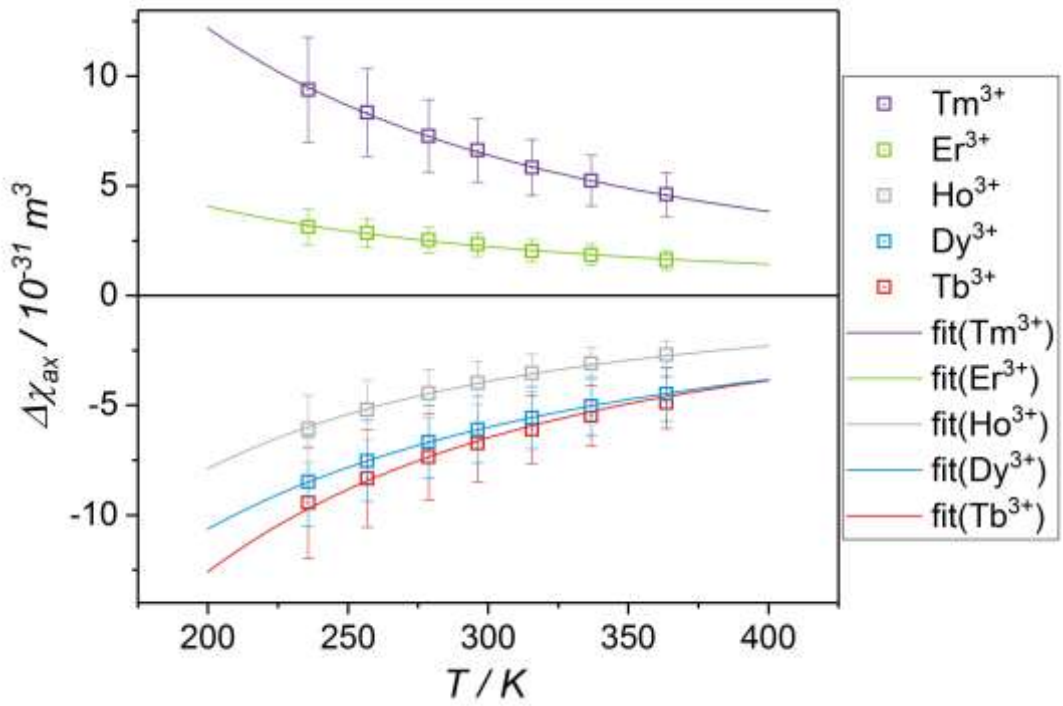

Figure 6: Comparison of experimental susceptibility anisotropies (data points) with those calculated from the set of ligand field parameters summarized in Table 2 (full lines).

10.1002/chem.201901388

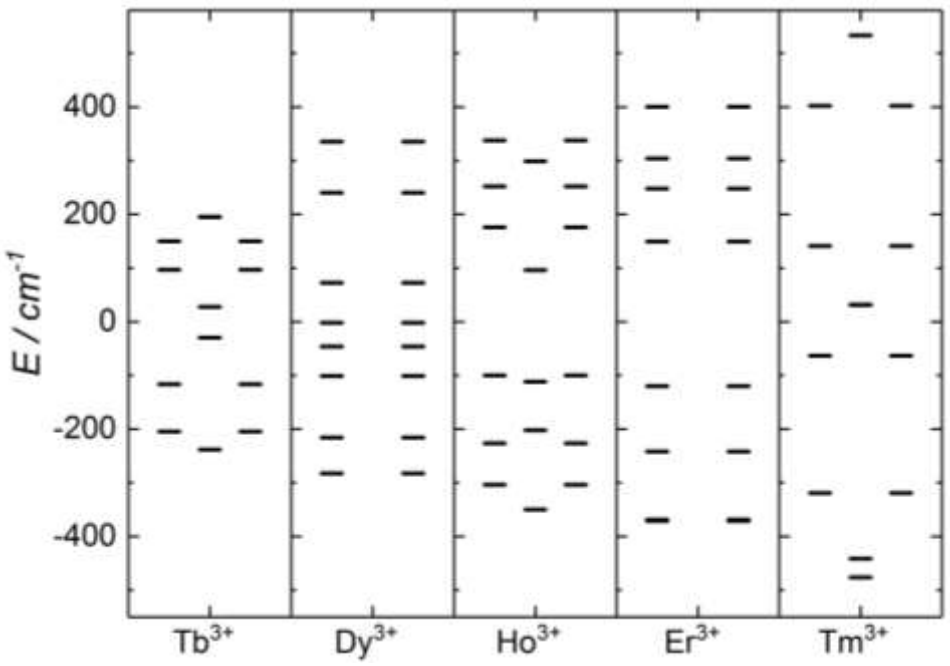

Figure 7: Relative energies of the wave functions ψ_i in **3** – **7**. Please note, that the lowest two Kramers doublets for the Er compounds **6** are very close in energy.

Conclusion

A series of neutral, six-coordinate and homoleptic lanthanide complexes with three additional ligand-centered unpaired electrons was synthesized. The neutral charge of the compounds results in excellent solubility in solvents of low polarity like toluene, and due to the large temperature range of liquid toluene, reliable magnetic coupling data could be extracted from paramagnetic solution NMR spectroscopy. The yttrium derivative allowed the NMR experimental determination of the inter-ligand coupling behavior of the anti-ferromagnetically coupled and thus spin-frustrated ligand environment with $J = -(96 \pm 1.5)$ cm^{-1}. NMR chemical shifts resulting from the paramagnetic ligand framework of the Y derivative were then subtracted from the observed chemical shifts of the other lanthanide complexes. This allowed the determination of the contributions of the paramagnetic lanthanide ions to the NMR shifts in the crystal field created by the three BIAN ligands. A simultaneous fitting of the ^{1}H NMR shifts of the complex series allowed the subsequent separation into Fermi-contact and

pseudocontact shifts induced by the unpaired f-electrons. The coupling between the unpaired electrons at the Ph-BIAN scaffold and the f-electrons at the Ln^{3+} centers leads to large Fermi-contact shifts at H atoms of the ligand. This observation is important for the enhancement of metal ligand interactions in the design of new magnetic materials. Subsequently, the temperature behavior of the NMR shifts and of residual quadrupolar couplings was determined as a basis for a ligand field parameter fitting. The ligand field is of predominantly equatorial type as described by the negative value of $A_2^0\langle r^2\rangle$. In such a system, the prolate ions Er^{3+} and Tm^{3+} are expected to exhibit easy-axis magnetic anisotropy., which is in agreement with the NMR data. The constitution of the individual wave functions indicates a significant mixing of m_J states for the Er derivative, while a non-degenerate ground state was derived for the Tm^{3+} ion.

Experimental Section

General

All reactions were carried out under standard Schlenk or Glovebox techniques. Anhydrous solvents were obtained from a MBRAUN SPS-800 solvent purification system. Deuterated toluene for NMR spectroscopy was dried by heating over K/benzophenone and distilled. Celite was heated for several hours to 140 °C under high vacuum to remove traces of moisture. NMR spectra were recorded on a Bruker AVANCE II NMR spectrometer (9.4 T, 400 MHz for ^{1}H) or a Bruker AVANCE III NMR spectrometer (15.1 T, 92.1 MHz for ^{2}H). The temperature controlling unit was calibrated using a standard substance (ethylene glycol in DMSO or methanol). Spectra were calibrated using the residual solvent resonance reported at 2.08 ppm.[32] Elemental analyses were carried out at the Microanalytical laboratory of the University Heidelberg using a vario MICRO cube (Elementar). Despite numerous attempts, the elemental analyses could not be improved beyond the reported values. The fact that the determined nitrogen content is lower than expected in all cases may indicate a systematic problem of combustion analyses of these compounds.

10.1002/chem.201901388

DFT calculations

All geometry optimizations and spin density calculations were carried out with the Gaussian 09 program suite (Rev. D.01)[33] applying the basis sets Stuttgart RSC Segmented/ECP[34] for Y^{3+} and 6-31g(d,p) for the remaining atoms. The solid-state structure of Ho(Ph-BIAN)$_3$ was chosen as the starting point of the calculations and Ho was replaced by Y. For the calculation of the spin densities of **1** with the various functionals, no symmetry restrictions were imposed.

Synthesis of Ph-BIAN

The ligand was synthesized according to known literature procedures. Direct reaction of acenaphthenequinone with aniline[35] produced only the monocondensation product. Hence, it was found necessary to synthesize the ligand *via* its $ZnCl_2$ adduct followed by removal of the metal.[36] All analytical data was identical to reported literature values.

Synthesis of D_{10}-Ph-BIAN

The partially deuterated ligand was synthesized according to the same procedure but employing D_5-aniline, which was prepared by modifications of literature syntheses. A detailed description can be found in the ESI.

Synthesis of Ln(Ph-BIAN)$_3$ **1** - **7**

Ph-BIAN (typically 100 mg, 301 µmol) was dissolved in anhydrous thf (5 mL) and K metal (typically 11.8 mg, 301 µmol, 1.0 eq.) was added. After stirring at room temperature overnight, the respective anhydrous lanthanide trichloride (100 µmol, 0.33 eq.) was added. The reaction was allowed to stir overnight before all volatile material was removed under reduced pressure. The residue was then extracted with toluene (5 mL), centrifuged and filtered. The solvent was removed under reduced pressure to yield a dark red solid, which was washed with a small amount of pentane.

The partially deuterated analogues **1D$_{30}$** – **7D$_{30}$** were synthesized in the same way employing the corresponding partially deuterated ligand in similar yields.

10.1002/chem.201901388

Y(Ph-BIAN)$_3$ (**1**)

Yield: 387 mg (356 µmol) from 500 mg Ph-BIAN, 71 %.

Elemental analysis: calcd. for $C_{72}H_{48}N_6Y$: C 79.62, H 4.45, N: 7.74; found: C 79.65, H 5.18, N 7.35.

Gd(Ph-BIAN)$_3$ (**2**)

Yield: 93 mg (81 µmol) from 100 mg Ph-BIAN, 80 %.

Elemental analysis: calcd. for $C_{72}H_{48}N_6Gd$: C 74.91, H 4.19, N: 7.28; found: C 73.88, H 4.77, N 6.91.

Tb(Ph-BIAN)$_3$ (**3**)

Yield: 65 mg (56 µmol) from 100 mg Ph-BIAN, 56 %.

Elemental analysis: calcd. for $C_{72}H_{48}N_6Tb$: C 74.80, H 4.18, N: 7.27; found: C 75.04, H 4.57, N 6.37.

Dy(Ph-BIAN)$_3$ (**4**)

Yield: 109 mg (94 µmol) from 101 mg Ph-BIAN, 93 %.

Elemental analysis: calcd. for $C_{72}DyH_{48}N_6$: C 74.57, H 4.17, N: 7.25; found: C 74.50, H 4.78, N 6.27.

Ho(Ph-BIAN)$_3$ (**5**)

Yield: 194 mg, (167 µmol) from 250 mg Ph-BIAN, 67 %.

Elemental analysis: calcd. for $C_{72}H_{48}HoN_6$: C 74.41, H 4.16, N: 7.23; found: C 73.82, H 4.75, N 6.36.

Er(Ph-BIAN)$_3$ (**6**)

Yield: 113 mg (97 µmol) from 100 mg Ph-BIAN, 97 %.

Elemental analysis: calcd. for $C_{72}ErH_{48}N_6$: C 74.26, H 4.15, N: 7.22; found: C 74.05, H 4.56, N 6.25.

Tm(Ph-BIAN)$_3$ (**7**)

Yield: 107 mg (92 µmol) from 100 mg Ph-BIAN, 92 %.

Elemental analysis: calcd. for $C_{72}H_{48}N_6Tm$: C 74.16, H 4.15, N: 7.21; found: C 74.05, H 4.49, N 6.92.

ACKNOWLEDGEMENTS

This work has been supported by the Fonds der Chemischen Industry with a Kekulé scholarship. The authors acknowledge support by the state of Baden-Württemberg through bwHPC and the German Research Foundation (DFG) through grant No. INST 40/467-1 FUGG.

REFERENCES

[1] a) R. Sessoli, H. L. Tsai, A. R. Schake, S. Wang, J. B. Vincent, K. Folting, D. Gatteschi, G. Christou, D. N. Hendrickson, *J. Am. Chem. Soc.* **1993**, *115*, 1804-1816; b) R. Sessoli, D. Gatteschi, A. Caneschi, M. A. Novak, *Nature* **1993**, *365*, 141-143.

[2] a) N. Ishikawa, M. Sugita, T. Ishikawa, S. Koshihara, Y. Kaizu, *J. Am. Chem. Soc.* **2003**, *125*, 8694-8695; b) C. A. P. Goodwin, F. Ortu, D. Reta, N. F. Chilton, D. P. Mills, *Nature* **2017**, *548*, 439-442; c) F. S. Guo, B. M. Day, Y. C. Chen, M. L. Tong, A. Mansikkamaki, R. A. Layfield, *Angew. Chem., Int. Ed.* **2017**, *56*, 11445-11449; d) F.-S. Guo, B. M. Day, Y.-C. Chen, M.-L. Tong, A. Mansikkamäki, R. A. Layfield, *Science* **2018**, *362*, 1400-1403; e) K. R. Meihaus, J. R. Long, *J. Am.*

Chem. Soc. **2013**, *135*, 17952-17957; f) S. K. Gupta, T. Rajeshkumar, G. Rajaraman, R. Murugavel, *Chem. Sci.* **2016**, *7*, 5181-5191.

[3] a) A. Abragam, B. Bleaney, *Electron Paramagnetic Resonance of Transition Ions*, Oxford University Press, **1970**; b) S.-D. Jiang, B.-W. Wang, S. Gao, in *Molecular Nanomagnets and Related Phenomena, Vol. 164*, Ch. 2, (Ed.: S. Gao), **2015**, pp. 111-143.

[4] a) J. Sievers, *Zeitschrift fur Physik B: Condensed Matter* **1982**, *45*, 289-296; b) J. D. Rinehart, J. R. Long, *Chem. Sci.* **2011**, *2*, 2078-2085.

[5] N. Ishikawa, M. Sugita, T. Okubo, N. Tanaka, T. Iino, Y. Kaizu, *Inorg. Chem.* **2003**, *42*, 2440-2446.

[6] L. Ungur, J. J. Le Roy, I. Korobkov, M. Murugesu, L. F. Chibotaru, *Angew. Chem., Int. Ed.* **2014**, *53*, 4413-4417.

[7] a) L. F. Chibotaru, in *Molecular Nanomagnets and Related Phenomena, Vol. 164*, Ch. 4, (Ed.: S. Gao), **2015**, pp. 185-231; b) L. Ungur, L. F. Chibotaru, *Inorg. Chem.* **2016**, *55*, 10043-10056.

[8] M. Perfetti, E. Lucaccini, L. Sorace, J. P. Costes, R. Sessoli, *Inorg. Chem.* **2015**, *54*, 3090-3092.

[9] a) N. Ishikawa, T. Iino, Y. Kaizu, *J. Phys. Chem. A* **2002**, *106*, 9543-9550; b) N. Ishikawa, *J. Phys. Chem. A* **2003**, *107*, 5831-5835; c) A. Santria, A. Fuyuhiro, T. Fukuda, N. Ishikawa, *Dalton Trans.* **2019**, 10.1039/C9DT00915A.

[10] a) S. Demir, J. M. Zadrozny, M. Nippe, J. R. Long, *J. Am. Chem. Soc.* **2012**, *134*, 18546-18549; b) S. Demir, M. Nippe, M. I. Gonzalez, J. R. Long, *Chem. Sci.* **2014**, *5*, 4701-4711; c) S. Demir, I.-R. Jeon, J. R. Long, T. D. Harris, *Coord. Chem. Rev* **2015**, *289–290*, 149-176; d) S. Demir, M. I. Gonzalez, L. E. Darago, W. J. Evans, J. R. Long, *Nat. Commun.* **2017**, *8*, 2144.

[11] a) I. Matei, T. Lixandru, *Buletinul Institutului Politehnic din Iaşi* **1967**, *13*, 245; b) M. H. Normant, *Comptes Rendus Acad. Sci. C* **1969**, *268*, 1811-1813.

[12] I. L. Fedushkin, A. A. Skatova, V. A. Chudakova, G. K. Fukin, *Angew. Chem., Int. Ed.* **2003**, *42*, 3294-3298.

[13] a) I. L. Fedushkin, O. V. Maslova, A. G. Morozov, S. Dechert, S. Demeshko, F. Meyer, *Angew. Chem., Int. Ed.* **2012**, *51*, 10584-10587; b) I. L. Fedushkin, O. V. Maslova, A. N. Lukoyanov, G. K. Fukin, *Comptes Rendus Chimie* **2010**, *13*, 584-592; c) I. L. Fedushkin, O. V. Maslova, E. V. Baranov, A. S. Shavyrin, *Inorg. Chem.* **2009**, *48*, 2355-2357; d) I. L. Fedushkin, O. V. Maslova, M. Hummert, H. Schumann, *Inorg. Chem.* **2010**, *49*, 2901-2910; e) I. L. Fedushkin, D. S. Yambulatov, A. A. Skatova, E. V. Baranov, S. Demeshko, A. S. Bogomyakov, V. I. Ovcharenko, E. M. Zueva, *Inorg. Chem.* **2017**, *56*, 9825-9833.

[14] J. Bendix, K. M. Clark, *Angew. Chem., Int. Ed.* **2016**, *55*, 2748-2752.

[15] I. Bertini, C. Luchinat, *Coord. Chem. Rev* **1996**, *150*, 77-110.

[16] A. A. Bothner-By, P. J. Domaille, C. Gayathri, *J. Am. Chem. Soc.* **1981**, *103*, 5602-5603.

[17] R. Shannon, *Acta Cryst. A* **1976**, *32*, 751-767.

[18] a) G. N. La Mar, W. D. Horrocks Jr, R. H. Holm, *NMR of Paramagnetic Molecules – Principles and Applications*, Academic Press, INC., New York and London, **1973**; b) I. Bertini;, C. Luchinat, in *Physical Methods for Chemists* (Ed.: R. S. Drago), Saunders College Publishing, **1992**; c) J. D. Satterlee, *Concepts in Magnetic Resonance* **1990**, *2*, 119-129.

[19] a) I. Bertini, C. Luchinat, G. Parigi, *Solution NMR of Paramagnetic Molecules. Applications to Metallobiomolecules and Models, Vol. 2*, Elsevier, **2001**; b) J. D. Satterlee, *Concepts in Magnetic Resonance* **1990**, *2*, 69-79.

[20] a) I. Bertini, C. Luchinat, G. Parigi, *Prog. Nuc. Magn. Res. Spectrosc.* **2002**, *40*, 249-273; b) J. A. Peters, J. Huskens, D. J. Raber, *Prog. Nuc. Magn. Res. Spectrosc.* **1996**, *28*, 283-350.

[21] V. S. Mironov, Y. G. Galyametdinov, A. Ceulemans, C. Görller-Walrand, K. Binnemans, *J. Chem. Phys.* **2002**, *116*, 4673-4685.

[22] a) R. M. Golding, M. P. Halton, *Aust. J. Chem.* **1972**, *25*, 2577-2581; b) C. N. Reilley, B. W. Good, R. D. Allendoerfer, *Anal. Chem.* **1976**, *48*, 1446-1458.

[23] P. J. Domaille, *J. Am. Chem. Soc.* **1980**, *102*, 5392-5393.

[24] R. Knorr, H. Hauer, A. Weiss, H. Polzer, F. Ruf, P. Löw, P. Dvortsák, P. Böhrer, *Inorg. Chem.* **2007**, *46*, 8379-8390.

[25] E. W. Bastiaan, C. Maclean, P. C. M. Van Zijl, A. A. Bothner, in *Annual Reports on NMR Spectroscopy, Vol. Volume 19* (Ed.: G. A. Webb), Academic Press, **1987**, pp. 35-77.

[26] Please note, that the value given by Knorr et. al. contains a typing error. The source cited by the authors gives the correct value.
[27] M. Hiller, M. Maier, H. Wadepohl, M. Enders, *Organometallics* **2016**, *35*, 1916-1922.
[28] C. Görller-Walrand, K. Binnemans, in *Handbook on the Physics and Chemistry of Rare Earths, Vol. 23*, Ch. 155, (Eds.: K. A. Gschneidner, L. Eyring), **1996**, pp. 121-283.
[29] K. W. H. Stevens, *Proc. Phys. Soc. A* **1952**, *65*, 209-215.
[30] M. Hiller, S. Krieg, N. Ishikawa, M. Enders, *Inorg. Chem.* **2017**, *56*, 15285-15294.
[31] a) M. Gerloch, R. F. McMeeking, *J. Chem. Soc. Dalton Trans.* **1975**, 2443-2451; b) J. H. Van Vleck, *The Theory of Electric and Magnetic Susceptibilities*, Oxford University Press, **1932**.
[32] G. R. Fulmer, A. J. M. Miller, N. H. Sherden, H. E. Gottlieb, A. Nudelman, B. M. Stoltz, J. E. Bercaw, K. I. Goldberg, *Organometallics* **2010**, *29*, 2176-2179.
[33] M. J. Frisch, G. W. Trucks, H. B. Schlegel, G. E. Scuseria, M. A. Robb, J. R. Cheeseman, G. Scalmani, V. Barone, B. Mennucci, G. A. Petersson, H. Nakatsuji, M. Caricato, X. Li, H. P. Hratchian, A. F. Izmaylov, J. Bloino, G. Zheng, J. L. Sonnenberg, M. Hada, M. Ehara, K. Toyota, R. Fukuda, J. Hasegawa, M. Ishida, T. Nakajima, Y. Honda, O. Kitao, H. Nakai, T. Vreven, J. J. A. Montgomery, J. E. Peralta, F. Ogliaro, M. Bearpark, J. J. Heyd, E. Brothers, K. N. Kudin, V. N. Staroverov, T. Keith, R. Kobayashi, J. Normand, K. Raghavachari, A. Rendell, J. C. Burant, S. S. Iyengar, J. Tomasi, M. Cossi, N. Rega, J. M. Millam, M. Klene, J. E. Knox, J. B. Cross, V. Bakken, C. Adamo, J. Jaramillo, R. Gomperts, R. E. Stratmann, O. Yazyev, A. J. Austin, R. Cammi, C. Pomelli, J. W. Ochterski, R. L. Martin, K. Morokuma, V. G. Zakrzewski, G. A. Voth, P. Salvador, J. J. Dannenberg, S. Dapprich, A. D. Daniels, O. Farkas, J. B. Foresman, J. V. Ortiz, J. Cioslowski, D. J. Fox, *Gaussian 09, Revision D.01*, Gaussian, Inc., Wallingford CT, **2013**.
[34] D. Andrae, U. Häußermann, M. Dolg, H. Stoll, H. Preuß, *Theor. Chim. Acta* **1990**, *77*, 123-141.
[35] C. D. Nunes, P. D. Vaz, V. Felix, L. F. Veiros, T. Moniz, M. Rangel, S. Realista, A. C. Mourato, M. J. Calhorda, *Dalton Trans.* **2015**, *44*, 5125-5138.
[36] C. S. K. Mak, H. L. Wong, Q. Y. Leung, W. Y. Tam, W. K. Chan, A. B. Djurišić, *J. Organomet. Chem.* **2009**, *694*, 2770-2776.

10.1002/chem.201901388

For Graphical Abstract

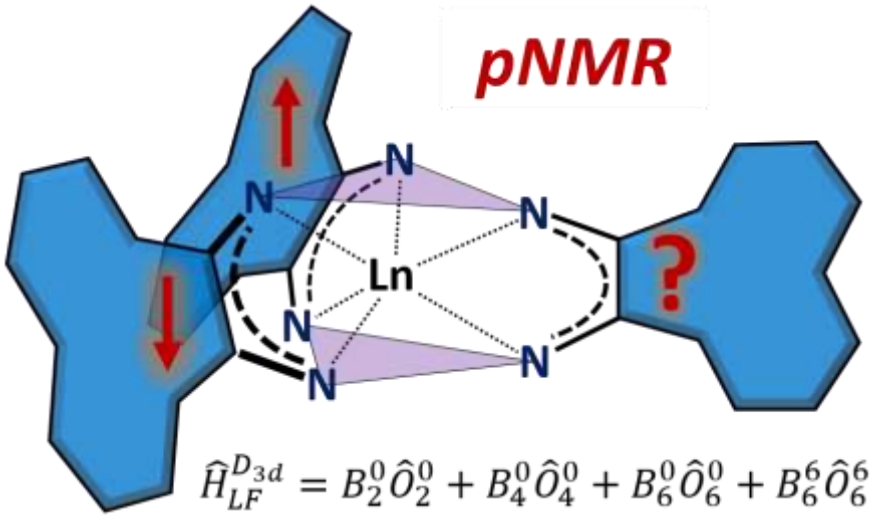

***3π + nf-electrons + Ligand Field*:** Magnetic anisotropy and J-coupling was measured by NMR spectroscopy in a new series of homoleptic Lanthanide complexes. Temperature dependent quadrupolar NMR splitting (RQC) and subsequent mathematical analysis describe the ligand field as equatorial with energy splitting of the m_J manifold up to 1000 cm^{-1}.